


Comparison of Smartphone Augmented Reality, Smartglasses Augmented Reality, and 3D CBCT-guided Fluoroscopy Navigation for Percutaneous Needle Insertion: A Phantom Study

Dilara J. Long¹ · Ming Li¹  · Quirina M. B. De Ruiters¹ · Rachel Hecht¹ · Xiaobai Li² · Nicole Varble^{1,3} · Maxime Blain¹ · Michael T. Kassin¹ · Karun V. Sharma⁴ · Shawn Sarin⁵ · Venkatesh P. Krishnasamy¹ · William F. Pritchard¹ · John W. Karanian¹ · Bradford J. Wood¹ · Sheng Xu¹

Received: 14 July 2020 / Accepted: 23 December 2020 / Published online: 6 January 2021

© This is a U.S. government work and not under copyright protection in the U.S.; foreign copyright protection may apply 2021

Abstract

Purpose To compare needle placement performance using an augmented reality (AR) navigation platform implemented on smartphone or smartglasses devices to that of CBCT-guided fluoroscopy in a phantom.

Materials and Methods An AR application was developed to display a planned percutaneous needle trajectory on the smartphone (iPhone7) and smartglasses (HoloLens1) devices in real time. Two AR-guided needle placement

systems and CBCT-guided fluoroscopy with navigation software (XperGuide, Philips) were compared using an anthropomorphic phantom (CIRS, Norfolk, VA). Six interventional radiologists each performed 18 independent needle placements using smartphone ($n = 6$), smartglasses ($n = 6$), and XperGuide ($n = 6$) guidance. Placement error was defined as the distance from the needle tip to the target center. Placement time was recorded. For XperGuide, dose-area product (DAP, $\text{mGy}\cdot\text{cm}^2$) and fluoroscopy time

✉ Ming Li
ming.li@nih.gov

Dilara J. Long
dilaralong@email.arizona.edu

Quirina M. B. De Ruiters
quirina.deruiters@nih.gov

Rachel Hecht
rachelhecht5@gmail.com

Xiaobai Li
xiaobai.li@nih.gov

Nicole Varble
nicole.varble@nih.gov

Maxime Blain
maxime.blain@nih.gov

Michael T. Kassin
michael.kassin@nih.gov

Karun V. Sharma
KVSharma@childrensnational.org

Shawn Sarin
ssarin@mfa.gwu.edu

Venkatesh P. Krishnasamy
vkpk27@gmail.com

William F. Pritchard
william.pritchard@nih.gov

John W. Karanian
john.karanian@nih.gov

Bradford J. Wood
bwood@nih.gov

Sheng Xu
xus2@cc.nih.gov

¹ Center for Interventional Oncology, Radiology and Imaging Sciences, Clinical Center, National Institutes of Health, Bethesda, MD 20892, USA

² Biostatistics and Clinical Epidemiology Service, Clinical Center, National Institutes of Health, Bethesda, MD 20892, USA

³ Philips Research of North America, Cambridge, MA 02141, USA

⁴ Sheikh Zayed Institute for Pediatric Surgical Innovation, Children's National Health System, Washington, DC, USA

⁵ Department of Interventional Radiology, George Washington University Hospital, Washington, DC, USA

(sec) were recorded. Statistical comparisons were made using a two-way repeated measures ANOVA.

Results The placement error using the smartphone, smartglasses, or XperGuide was similar (3.98 ± 1.68 mm, 5.18 ± 3.84 mm, 4.13 ± 2.38 mm, respectively, $p = 0.11$). Compared to CBCT-guided fluoroscopy, the smartphone and smartglasses reduced placement time by 38% ($p = 0.02$) and 55% ($p = 0.001$), respectively. The DAP for insertion using XperGuide was 3086 ± 2920 mGy*cm², and no intra-procedural radiation was required for augmented reality.

Conclusions Smartphone- and smartglasses-based augmented reality reduced needle placement time and radiation exposure while maintaining placement accuracy compared to a clinically validated needle navigation platform.

Keywords Augmented reality · Interventional radiology · Image guidance · Percutaneous needle biopsy · Smartphone · HoloLens · Smartglasses · CBCT fluoroscopy · XperGuide

Introduction

Safe and accurate percutaneous needle biopsies are dependent on precise treatment planning and intra-procedural imaging guidance. Cone beam CT (CBCT)-guided fluoroscopic navigation (XperGuide, Philips Healthcare, Best, The Netherlands) incorporates virtual needle path planning on CBCT images, automatically defines projections for entry or bull's-eye view along the axis of the needle path and orthogonal progress views, and superimposes the three-dimensional registered trajectory on fluoroscopic images [1]. The technique has been shown to have diagnostic efficacy and higher needle placement accuracy compared to CT alone, but comes with a cost of increased radiation [2–5]. Moreover, the display of the needle trajectory away from the patient on a monitor requires the operator to rely heavily on memory, visuospatial skills, hand–eye coordination, and clinical training and experience [6]. Easier access to a treatment plan within the operator's line of sight could facilitate or standardize percutaneous needle interventions. [7, 8].

Augmented reality (AR) is an emerging navigational tool in interventional radiology that may provide accurate and reproducible needle guidance while reducing radiation exposure [8–13]. AR describes the superimposition of digital information onto a display using stationary, handheld, or head-mounted devices [8]. The overlay of 3D

treatment information directly onto the procedural environment rather than a remote monitor may facilitate more intuitive appreciation of anatomy, treatment plans, and execution [14]. The direct line of sight and real-time access to digital patient information has the potential to improve standardization and reproducibility, reduce inter-user variability, and shorten learning curves [8, 15].

A novel AR navigation platform was developed to guide percutaneous needle placements, enabling needle trajectory planning and visualization on handheld or wearable devices [16, 17]. Prior work with this software showed comparable image overlay accuracy between the smartphone and smartglasses devices [16]. In addition, performance using the AR smartphone showed significant improvement in needle placement accuracy, procedure time, and radiation exposure compared to CT freehand insertion [17]. The AR devices are similar to CBCT-guided fluoroscopy, enabling needle insertions in oblique planes by providing entry and progress views for guidance without the need for additional technology, e.g., electromagnetically tracked needles. This study compared percutaneous needle placement performance using the AR smartphone, AR smartglasses, and CBCT-guided fluoroscopy in a phantom.

Materials and Methods

Phantom

An anthropomorphic abdominal phantom (CIRS Model 057A, Norfolk, VA) (Fig. 2A) with self-healing properties allowed repeated needle insertions with CT-visible target lesions (Fig. 1A). The lesions targeted ($n = 6$) had diameters ranging from 6.5 to 13.5 mm. Needle entry points ($n = 6$) were selected at random locations on the anterior surface to include a variety of insertion depths (mean 71.7 ± 16.7 mm, range 56.0–102.4 mm) and polar angles (mean $38.2 \pm 7.1^\circ$, range 31.6–50.9°). All needle trajectories were double-angled with craniocaudal angulation and rotation about the z-axis. Six 2-mm metal spheres were placed on the phantom surface to identify needle entry points on pre-procedural CT imaging.

AR Components

An orientation reference marker ($10 \times 5 \times 5$ cm) was 3D printed with metal fiducials embedded at each corner for identification on pre-procedural CT imaging and subsequent registration. An image with no repetitive patterns was affixed to its surface for recognition by the AR device camera and application. The marker was rigidly attached to the phantom and kept within view of the device camera by the operator during use. This enabled automatic registration

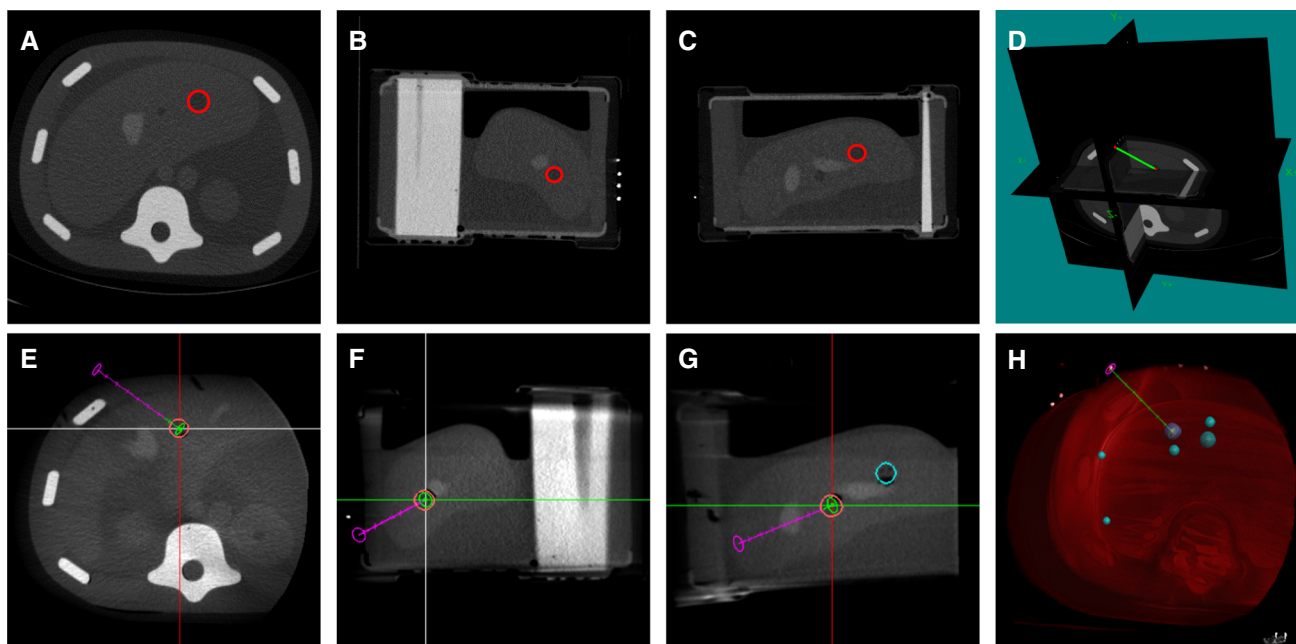


Fig. 1 Pre-procedural planning as shown on the augmented reality (AR) (A–D) and CBCT-guided fluoroscopy (E–H) software. A–C Axial, sagittal, and coronal CT views of the abdominal phantom in the AR software, with the segmented target (red circle). D The phantom in 3D space with the needle path (green line) and entry point and target (red dots). E–G The axial, sagittal, and coronal views of the

phantom in the CBCT-guided fluoroscopy software show the planned needle trajectory (purple line), entry point (purple circle), needle endpoint (green circle), and the segmented target (orange). H The surface rendering of the phantom with the CBCT-guided fluoroscopy needle trajectory (green), the entry point (purple circle) and the needle target (green circle) within the segmented target (dark blue)

between preoperative CT images and the phantom in actual space (Fig. 2B).

The AR devices were the iPhone 7 (Apple, Cupertino, CA, USA) and HoloLens 1 (Microsoft, Redmond, WA, USA); however, the AR application [16] is compatible with smartphone or smartglasses devices that run on iOS, Windows or Android. The AR application enabled automatic registration and real-time superimposition of the selected needle trajectory onto the image of the phantom. The smartphone displayed the planned needle trajectory as an overlay on the real-time image of the phantom on the smartphone screen (Fig. 2A–C). The smartphone was operated using the touchscreen with needle trajectory selection from a drop-down menu. The smartglasses superimposed the planned needle trajectory onto the 3D environment (Fig. 2D–E). The AR application, including selection of needle trajectory, was operated by hand gestures and voice commands.

Image Acquisition, Processing, and Pre-procedural Planning

AR-guided procedures

A pre-procedural CT scan (Brilliance MX8000 IDT 16-section Detector CT; Philips, Cleveland, OH USA) of the phantom and reference marker was acquired prior to

each set of six interventions with each device (3.0 mm sections at 1.5 mm intervals; 120 kVp; 275 mAs; 30 cm field of view). Treatment planning was performed as previously described with the custom application running on a personal computer (Microsoft Surface Pro, Redmond, WA, USA) (Fig. 1A–D) [16, 17]. Briefly, six targets were segmented. A unique target center and surface entry point pair was selected to define and generate each needle trajectory. The fiducials at the corners of the reference marker were identified, enabling point-to-point based rigid registration of the preoperative CT and trajectories to the real 3D marker in actual space. All six needle trajectories were uploaded for subsequent display by the AR device [17]. The same paired targets and entry points were used for all operators.

CBCT-guided fluoroscopic procedures

A CBCT scan was acquired (Allura Xper FD20 X-ray System, Philips, Best, The Netherlands) at 120 kVp. The needle guidance platform (XperGuide) was used for treatment planning and execution on an interventional workstation (OncoSuite, Philips) (Fig. 1E–H). Since the phantom targets were not optimally visualized on CBCT, a CT scan of the phantom was imported and rigidly and automatically registered to the CBCT. The targets and entry points were selected, defining the trajectories. This

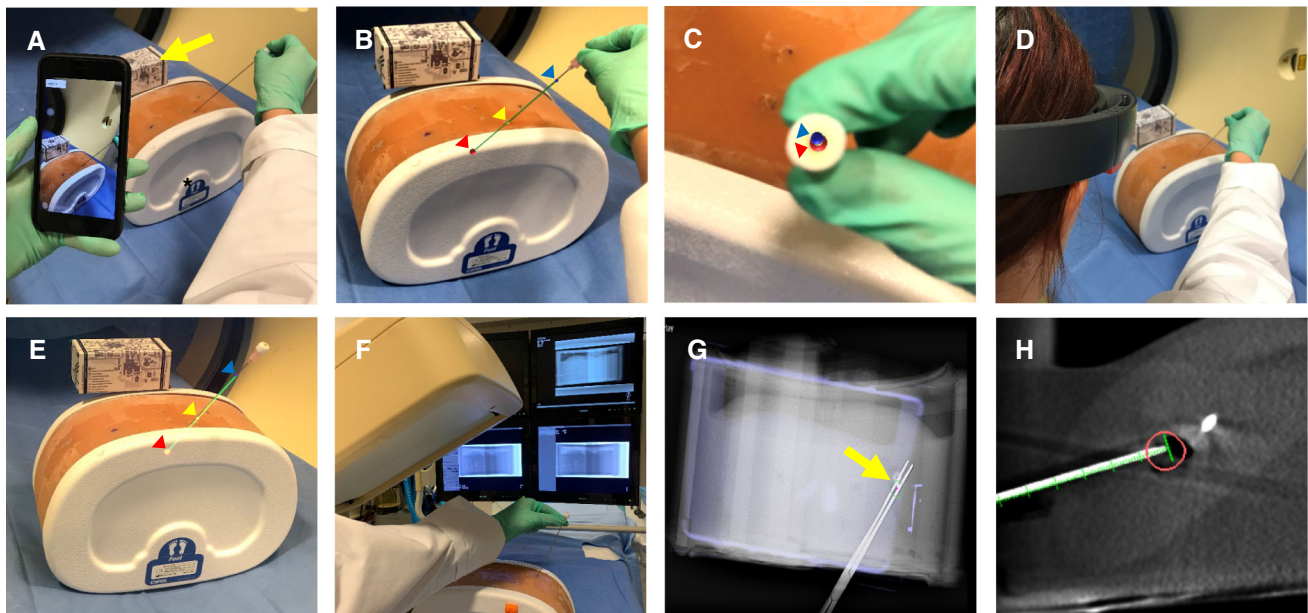


Fig. 2 Experimental workflow with augmented reality (AR) smartphone, smartglasses and CBCT-guided fluoroscopy. **A** The phantom (asterisk) and the 3D reference marker (yellow arrow) were maintained in the smartphone field of view during needle insertion. **B** Screenshot of the AR smartphone application showed the needle and superimposed virtual needle path (green line), target (red dot, identified by the red arrowhead), entry point (yellow dot, identified by the yellow arrowhead), and final virtual position of the proximal end of the needle (blue dot, identified by the blue arrowhead). **C** Screenshot of the smartphone application that showed the bull's-eye view used to guide the initial needle puncture and insertion with the target (red dot identified by the red arrowhead), proximal needle end marker (blue dot, identified by the blue arrowhead) and needle hub center overlapped. **D** AR smartglasses-guided needle placement. **E** Image

defined set of trajectories was imported into CBCT images subsequently acquired for each operator, and automatically registered. Overlay modifications, e.g., entry points, could be made manually. The 3D needle trajectories were registered to the fluoroscopic image for monitoring needle insertion.

Phantom Procedure Protocol

Six operators with 3–25 years clinical experience (5 interventional radiologists and one interventional radiology resident) each used the AR smartphone ($n = 6$), AR smartglasses ($n = 6$), and CBCT-guided fluoroscopic ($n = 6$) navigation systems for a total of 18 independent insertions with Hawkins-Akins 18G needles (Cook, Bloomington, IN, USA). The order of use of the two AR devices was randomized for each operator. CBCT-guided fluoroscopic navigation was performed last. The order of insertion for the needle trajectories was randomized among operators, with each operator performing 6 consecutive needle placements using each device. Operators practiced

acquired from behind the lens of the AR smartglasses depicting the augmentation shown in the AR application with the needle path (green), target (red dot, identified by red arrowhead), entry point (yellow dot, identified by yellow arrowhead), and the final virtual position of the proximal needle (blue dot, identified by blue arrowhead). **F** CBCT-guided fluoroscopy navigation with last fluoroscopy images (plain fluoroscopy and CBCT-guidance fluoroscopy overlay) shown in the monitors. **G** CBCT-guided fluoroscopy entry view during initial needle puncture and advancing of needle, aligning the needle shaft with the entry point (green circle) and trajectory (purple dot). **H** Orthogonal progress view with the virtual needle trajectory overlying the needle shaft and the needle tip at the correct depth

(< 15 min) prior to the use of each device and reviewed the treatment plan for each needle trajectory prior to insertion. Operators were instructed to insert the needle into each target center as accurately as possible, within a reasonable amount of time. Needle insertion time was measured from the initial puncture until operator satisfaction with final position. After placement of three needles, a CT scan was acquired for later measurement of placement error and the needles were then removed.

For AR smartphone-guided procedures, the smartphone was held in one hand while the other was used to insert the needles (Fig. 2A, B). With the needle at the entry point, the entry view along the axis of the trajectory was used to guide needle puncture (Fig. 2C). Proper alignment was assessed by observing that the needle coincided with the superimposed virtual trajectory, in which the proximal and distal ends were marked by blue and red dots, respectively. Moving the smartphone about the phantom enabled visualization of needle progress and virtual accuracy, and guided adjustments (Fig. 2A, B). For AR smartglasses-guided procedures, the operator fastened the device to their

head and performed a brief ocular calibration (1–2 min) (Fig. 2D). The entry view could be viewed with one eye closed, using a single line of sight in a single frame of the smartglasses. Needle progress was visualized by orienting the smartglasses to various positions and perspectives about the phantom. Operators were polled on relative confidence of use, advantages, and frustrations with each device.

For CBCT-guided fluoroscopic procedures, the operator used the entry view to align the needle at the entry point and advance it into the phantom. Intermittent C-arm rotation to orthogonal progress views showed needle insertion depth and alignment. Rapid rotation between the views was repeated with needle manipulation until placement was satisfactory. Dose-area product (DAP, $\text{mGy}\cdot\text{cm}^2$) and fluoroscopy time (sec) were recorded for each placement.

Post-procedural Measurement

Needle placement error was defined as the distance (mm) from the needle tip to the target center. AR-guided needle placement error was calculated (Fig. 3A) using an open source DICOM viewer (OsiriX Lite v.11.0.2, Geneva, Switzerland), based on the 3D coordinates of the needle tip and target. CBCT-guided fluoroscopic needle placement error was measured using XperGuide, where the end of the planned trajectory identified the target center. The orthogonal lateral error (Fig. 3B) and in-direction error (Fig. 3C) relative to the target center were measured, and total distance was then calculated using the quadratic equation. Since XperGuide error was based on the distance between the needle tip and the end of the needle trajectory, the measurement was not affected by any initial registration errors between the CBCT and CT.

Statistical Analysis

Prism was used for statistical analyses (GraphPad Software, version 8.0, La Jolla, CA). A two-way analysis of variance with repeated measures of targets was used to compare the main effects of operator ($n = 6$) and device ($n = 3$) as well as their interaction effect on placement error and time. The effect of target on performance was also analyzed. A post hoc Tukey's multiple comparisons test was used to make statistical comparisons between groups. An alpha of 0.05 was used for all statistical comparisons. Descriptive statistics were presented as mean \pm SD.

Results

Mean needle placement errors using the AR smartphone, AR smartglasses, and CBCT-guided fluoroscopy were 3.98 ± 1.68 mm, 5.18 ± 3.84 mm, and 4.13 ± 2.38 mm, respectively ($p = 0.096$, Fig. 4A). Interaction effects between operator and device were observed ($p = 0.01$). Post hoc comparisons within operators showed that one operator with 18 years of experience placed needles with less error using XperGuide compared to AR smartphone ($p = 0.032$) and AR smartglasses ($p = 0.016$). Post hoc comparisons within devices showed that the same operator placed needles with less error when using XperGuide compared to an operator with 5 years of experience ($p = 0.009$). The remainder of post hoc comparisons showed p values greater than 0.05.

Mean needle placement times using the AR smartphone, AR smartglasses, and CBCT-guided fluoroscopy were 94.8 ± 28.3 s, 68.5 ± 42.6 s, and 152.0 ± 118.8 s, respectively ($p = 0.003$, Fig. 4B). Interaction effects between operator and device were not observed

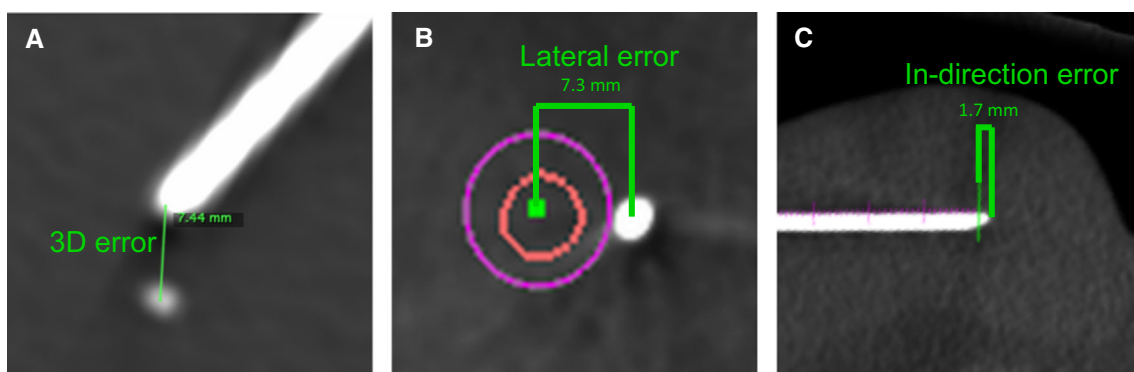
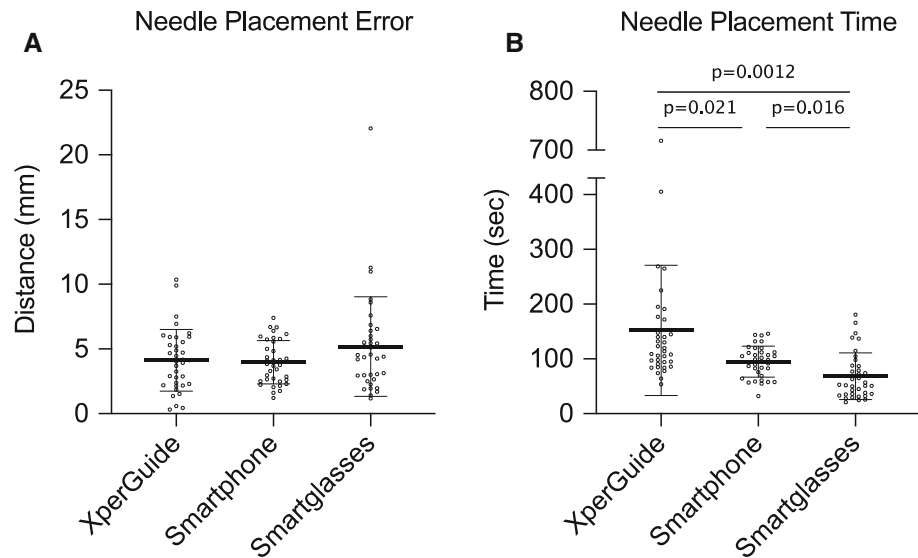


Fig. 3 Postoperative measurement of the needle placement error for augmented reality (AR) and CBCT-guided fluoroscopy. **A** AR needle placement error was acquired selecting a CT reconstruction plane that included the needle and target. Placement error was measured from the needle tip to the target center. **B** Lateral error in the entry point

view using CBCT-guided fluoroscopy. **C** In-directional error in the progress view using CBCT-guided fluoroscopy. The total error from the needle tip to the target center for CBCT-guided fluoroscopy was calculated using the quadratic formula

Fig. 4 Needle placement error and time for all operators. **A** Scatter dot plot of the needle placement error (mean \pm SD). The placement errors for each device were similar. **B** Scatter dot plot of the mean needle placement time (mean \pm SD). The placement time for the augmented reality (AR) smartphone was less than for CBCT-guided fluoroscopy ($p = 0.021$). The time for AR smartglasses was less than for AR smartphone ($p = 0.016$) and CBCT-guided fluoroscopy ($p = 0.0012$)



($p = 0.063$). The use of the AR smartphone and AR smartglasses reduced needle placement time by 38% ($p = 0.02$) and 55% ($p = 0.001$), respectively, compared to CBCT-guided fluoroscopy. AR smartglasses-guided needle placements showed a reduced placement time compared to the smartphone ($p = 0.016$). The needle trajectory had no observable association with placement error ($p = 0.39$) or time ($p = 0.76$).

Most operators reported more confidence using the smartphone than the smartglasses, in part due to fewer minor malfunctions. The camera view of the reference marker was more likely to be obstructed by the smartglasses operator's free hand which led to the loss of image registration and the AR display. In contrast to the hands-free smartglasses, ergonomics of smartphone use were challenged by the requirement of holding the smartphone in position with one hand while advancing the needle with the other. The operator also shifted gaze between the patient to the iPhone. One operator found a solution by keeping both hands in contact with the phone to stabilize the complex system (Fig. 5). A few operators reported mild headache and dizziness with the smartglasses.

For CBCT-guided fluoroscopy, the mean DAP was 3086 ± 2920 mGy*cm² with 55 ± 59 s of fluoroscopic radiation.

Discussion

Needles were placed with comparable accuracy using 3 different percutaneous navigation platforms, the AR smartphone, AR smartglasses, and CBCT-guided fluoroscopic navigation. Both AR guidance techniques had accurate placement while reducing needle placement time

and intra-procedural radiation exposure, which is inherent to CBCT-guided fluoroscopy.

The AR platform showed improvements in ergonomics and inter-user variability compared to CBCT-guided fluoroscopy, without major alterations in workflow. Compared to the AR devices, the bulk of the C-arm can limit selection of needle trajectories during planning and the operator's freedom of movement. All operators had clinical experience with fluoroscopically guided needle placement, while the AR platforms are not in clinical use. Despite having less than 15 min to practice with each AR platform, performance using the AR platforms matched or exceeded that of CBCT-guided placement. The presented AR platforms have the potential to reduce learning curves as well as variability in performance among users with differing levels of experience. Further evaluation with AR navigation is needed to determine whether complication rates and diagnostic accuracy correlate with experience, as they do for CBCT-guided percutaneous needle biopsies [6].

The AR smartphone and smartglasses showed comparable needle placement accuracy, but with different technical and ergonomic factors. With smartphone use, the operator's focus shifted between the display and the patient, as with CBCT-guided fluoroscopy. In contrast, smartglasses offered the advantage of a direct line of sight through the lens display with a more intuitive, hands-free user experience [14]. However, a few operators reported symptoms of cybersickness which is commonly associated with immersive technology [18, 19]. The smartglasses also required user-dependent calibration and adjustment, which could hamper workflow.

There were limitations to this work. The study used a stationary phantom constructed of homogenous material which does not reflect the full complexity of motion and

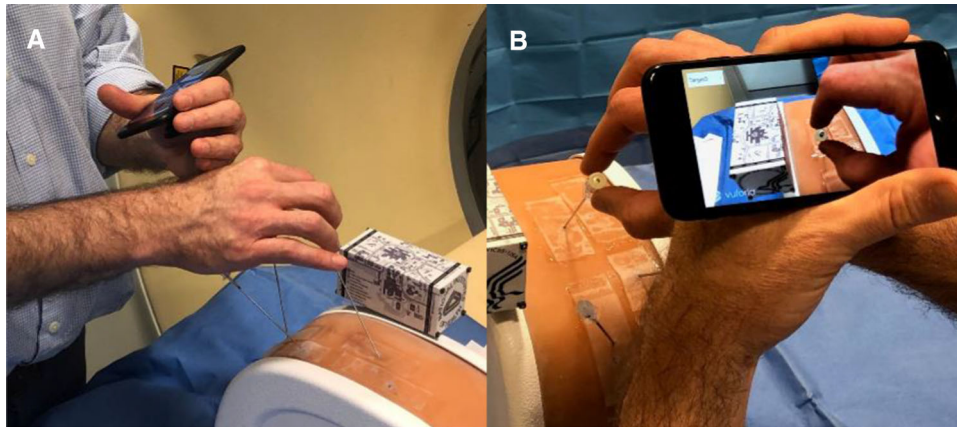


Fig. 5 Needle stabilization technique for smartphone-guided needle placement. **A** The two hands were kept in contact with the hand holding the smartphone resting on top of the hand guiding the needle, fixing the relationships, and stabilizing needle insertion. **B** The actual

tissue properties. While AR technology does not require intra-procedural radiation, one also loses the ability to monitor and adjust for respiratory deformation or needle deviation that is provided by fluoroscopic imaging. AR systems could be improved with integration of motion tracking [20–22], elastic registration [23], and needle shape reconstruction to account for needle bending [24]. AR smartphone or smartglasses technology could be used in conjunction with CBCT-guided fluoroscopy to take advantages of the strengths and mitigate the shortcomings of both approaches. For example, AR has been implemented in combination with CBCT-guided fluoroscopy with cameras on the detector to reduce radiation exposure while maintaining accuracy [20].

Conclusion

An AR platform using a smartphone or smartglasses showed needle placement accuracy comparable to CBCT-guided fluoroscopy while reducing procedure time and radiation exposure in a stationary phantom. This AR platform may benefit less experienced operators or serve as a platform for physician training or standardization. While there may be ergonomic and technical advantages to using AR smartphone or smartglasses, future refinements should be made to both devices to define and enhance clinical value in specific interventional applications.

Funding This work was supported by the Center for Interventional Oncology in the Intramural Research Program of the National Institutes of Health (NIH) by intramural NIH Grants NIH Z01 1ZID BC011242 and CL040015.

Compliance with Ethical Standards

needle axis was positioned in line with the virtual needle trajectory in the bull's-eye view. This method reduced the need to shift the line of sight back and forth from the display to the phantom

Conflict of interest NIH has a Cooperative Research and Development Agreements with Philips Research, Celsion Corp, Biocompatibles UK Ltd–Boston Scientific Corporation, Siemens Medical Solutions, NVIDIA, and XAct Robotics. None of these entities were involved in the reported work. NV is an employee of Philips Research North America. The content of this manuscript does not necessarily reflect the views, policies, or opinions of the U.S. Department of Health and Human Services. The mention of commercial products, their source, or their use in connection with material reported herein is not to be construed as an actual or implied endorsement of such products by the United States Government. Opinions expressed are those of the authors, not necessarily the NIH.

Ethical Approval This article does not contain any studies with human participants or animals performed by any of the authors.

Informed Consent For this type of study, informed consent is not required.

Consent for Publication For this type of study, consent for publication is not required.

References

1. Racadio JM, Babic D, Homan R, Rampton JW, Patel MN, Racadio JM, et al. Live 3D guidance in the interventional radiology suite. *AJR Am J Roentgenol.* 2007;189(6):W357–64.
2. Busser WM, Braak SJ, Futterer JJ, van Strijen MJ, Hoogeveen YL, de Lange F, et al. Cone beam CT guidance provides superior accuracy for complex needle paths compared with CT guidance. *Br J Radiol.* 2013;86(1030):20130310.
3. Floridi C, Reginelli A, Capasso R, Fumarola E, Pesapane F, Barile A, et al. Percutaneous needle biopsy of mediastinal masses under C-arm conebeam CT guidance: diagnostic performance and safety. *Med Oncol.* 2017;34(4):67.
4. Fior D, Vacirca F, Leni D, Pagni F, Ippolito D, Riva L, et al. Virtual guidance of percutaneous transthoracic needle biopsy with C-arm cone-beam CT: diagnostic accuracy, risk factors and effective radiation dose. *Cardiovasc Intervent Radiol.* 2019;42(5):712–9.

5. Braak SJ, van Strijen MJ, van Leersum M, van Es HW, van Heesewijk JP. Real-Time 3D fluoroscopy guidance during needle interventions: technique, accuracy, and feasibility. *AJR Am J Roentgenol.* 2010;194(5):W445–51.
6. Ahn SY, Park CM, Yoon SH, Kim H, Goo JM. Learning curve of C-arm cone-beam computed tomography virtual navigation-guided percutaneous transthoracic needle biopsy. *Korean J Radiol.* 2019;20(5):844–53.
7. Wood BJ, Locklin JK, Viswanathan A, Kruecker J, Haemmerich D, Cebal J, et al. Technologies for guidance of radiofrequency ablation in the multimodality interventional suite of the future. *J Vasc Interv Radiol.* 2007;18(1 Pt 1):9–24.
8. Park BJ, Hunt SJ, Martin C, Nadolski GJ, Wood BJ, Gade TP. Augmented and mixed reality: technologies for enhancing the future of IR. *J Vasc Interv Radiol.* 2020;31:1074–82.
9. Uppot RN, Laguna B, McCarthy CJ, De Novi G, Phelps A, Siegel E, et al. Implementing virtual and augmented reality tools for radiology education and training, communication, and clinical care. *Radiology.* 2019;291(3):570–80.
10. Kennigott HG, Preukschas AA, Wagner M, Nickel F, Muller M, Bellemann N, et al. Mobile, real-time, and point-of-care augmented reality is robust, accurate, and feasible: a prospective pilot study. *Surg Endosc.* 2018;32(6):2958–67.
11. Heinrich F, Joeres F, Lawonn K, Hansen C. Comparison of projective augmented reality concepts to support medical needle insertion. *IEEE Trans Vis Comput Graph.* 2019;25(6):2157–67.
12. Solbiati M, Passera KM, Rotilio A, Oliva F, Marre I, Goldberg SN, et al. Augmented reality for interventional oncology: proof-of-concept study of a novel high-end guidance system platform. *Eur Radiol Exp.* 2018;2:18.
13. Elsayed M, Kadom N, Ghobadi C, Strauss B, Al Dandan O, Aggarwal A, et al. Virtual and augmented reality: potential applications in radiology. *Acta Radiol.* 2020. <https://doi.org/10.1177/0284185119897362>.
14. Pratt P, Ives M, Lawton G, Simmons J, Radev N, Spyropoulou L, et al. Through the HoloLens looking glass: augmented reality for extremity reconstruction surgery using 3D vascular models with perforating vessels. *Eur Radiol Exp.* 2018;2(1):2.
15. Barsom EZ, Graafland M, Schijven MP. Systematic review on the effectiveness of augmented reality applications in medical training. *Surg Endosc.* 2016;30(10):4174–83.
16. Li M, Seifabadi R, Long D, De Ruiter Q, Varble N, Hecht R, et al. Smartphone- versus smartglasses-based augmented reality (AR) for percutaneous needle interventions: system accuracy and feasibility study. *Int J Computer Assist Radiol Surg.* 2020;15:1921–30.
17. Hecht R, Li M, de Ruiter QMB, Pritchard WF, Li X, Krishnasamy V, et al. Smartphone augmented reality CT-based platform for needle insertion guidance: a phantom study. *Cardiovasc Intervent Radiol.* 2020;43:756–64.
18. Vovk A, Wild F, Guest W, Kuula T, editors. *Simulator Sickness in Augmented Reality Training Using the Microsoft HoloLens. Conference on Human Factors in Computing Systems*; 2018; Montreal, Canada. New York, NY United States: Association for Computing Machinery, New York, NY; 2018.
19. Rebenitsch L, Owen C. Review on cybersickness in applications and visual displays. *Virtual Real.* 2016;20(2):101–35.
20. Racadio JM, et al. Augmented reality on a C-arm system: a preclinical assessment for percutaneous needle localization. *Radiology.* 2016;281:249–55.
21. Nicolau SA, Pennec X, Soler L, Buy X, Gangi A, Ayache N, et al. An augmented reality system for liver thermal ablation: design and evaluation on clinical cases. *Med Image Anal.* 2009;13(3):494–506.
22. Fichtinger G, Deguet A, Masamune K, Balogh E, Fischer GS, Mathieu H, et al. Image overlay guidance for needle insertion in CT scanner. *IEEE Trans Biomed Eng.* 2005;52(8):1415–24.
23. Si W, Liao X, Qian Y, Wang Q. Mixed reality guided radiofrequency needle placement: a pilot study. *IEEE Access.* 2018;6:31493–502.
24. Lin MA, Siu AF, Bae JH, Cutkosky MR, Daniel BL. HoloNeedle: augmented reality guidance system for needle placement investigating the advantages of three-dimensional needle shape reconstruction. *IEEE Robot Autom Lett.* 2018;3(4):4156–62.

Publisher's Note Springer Nature remains neutral with regard to jurisdictional claims in published maps and institutional affiliations.